Effect of pitch distance of rotational twisted tape on the heat transfer and fluid flow characteristics

Hossein Arasteh[1], Alireza Rahbari[2], Ramin Mashayekhi[3], Amir Keshmiri[4], Roohollah Babaei Mahani[5,6], Pouyan Talebizadehsardari[7,*]

[1] Department of Mechanical Engineering, Isfahan University of Technology, Isfahan, Iran

[2] Research School of Electrical, Energy and Materials Engineering, The Australian National University, Canberra ACT 2601, Australia

[3] Research & Development Team, Couette Limited, Altrincham, UK.

[4] Department of Mechanical, Aerospace and Civil Engineering (MACE), The University of Manchester, Manchester, M13 9PL, UK.

[5] Institute of Research and Development, Duy Tan University, Da Nang 550000, Vietnam.

[6] Faculty of Civil Engineering, Duy Tan University, Da Nang 550000, Vietnam.

[7] Centre for Sustainable Energy Use in Food Chains, Institute of Energy Futures, Brunel University London, Kingston Lane, Uxbridge, Middlesex, UB8 3PH, UK

Abstract

A numerical simulation study on the laminar convective heat transfer and fluid flow characteristics in a plain tube equipped with stationary and rotating twisted tapes are performed in this study. Three angular velocities, three twisted tape pitches and four Reynolds numbers ranging from 250 to 1000 are investigated. The numerical results show that using the twisted tape insert increases the heat transfer, friction coefficient and energy consumption (including pumping power and motor power to drive the rotating twisted tape). Higher enhancement is achieved as the twisted tape starts to rotate and its pitch reduces. As the twisted tape starts to rotate, decreasing its pitch does not change the heat transfer rate significantly. As a result applying more angular velocity is not rational and leads to more energy consumption. It is also found that applying a rotating twisted tape instead of a stationary twisted tape is only practical

* Corresponding author.

E-mail address: pouyan.talebizadehsardari@brunel.ac.uk (Pouyan Talebizadehsardari).

and beneficial in low Reynolds numbers, in the viewpoint of energy saving. The highest dimensionless number of performance evaluation criterion corresponds to the case of stationary twisted tape at Reynolds number of 1000 and twisted tape pitch of L/6 which is equal to 1.50.

Keywords: Rotating twisted tape; Pitch investigation; Secondary flow; Energy saving.

Nomenclature

A	area (m^2)	**Greek symbols**	
C_p	specific heat coefficient (J/kgK)	μ	dynamic viscosity (Pa s)
D	pipe diameter (m)	ϑ	kinematic viscosity (m^2/s)
f	friction coefficient	ρ	density (kg/m^3)
F	Total pressure and viscos forces	ω	twisted tape angular velocity (1/s, rad/s)
h	heat transfer coefficient (W/m^2K)	τ	torque (kgm^2/s^2)
k	conductivity (W/mK)	**Subscripts**	
L	length (m)	avg	average
Nu	Nusselt number	b	bulk
p	pressure (Pa)	f	fluid
P	twisted tape pitch	s	plain tube
Re	Reynolds number	**Acronyms**	
T	temperature (K)	PEC	performance evaluation criterion
V	velocity vector (m/s)	PT	plain tube
$\dot{W}_p$	pumping power (W)	RTT	rotating twisted tape
$\dot{W}_m$	motor power (W)	STT	stationary twisted tape
$\dot{E}_c$	energy consumption (W)		

1. Introduction

Convective heat transfer plays a key role in numerous industries and engineering systems, including solar systems [1], fuel cells [2], air conditioning equipment [3], thermoelectric cooling [4], heat sinks [5], etc [6], [7]. Therefore, enhancing this mode of heat transfer has been the focus of several researchers, consequently, various methods have been proposed in the last two decades. Among these techniques, increasing the mixing flow effects by inserting different types of solids in various configurations such as twisted tapes, and also modifying the

characteristics of the working fluid by dispersing nanoparticles in the base fluid (known as nanofluid [6-8]) have proven to be efficient methods to improve the thermal performance of engineering systems.

So far, different types of twisted tape inserts have been used for convective heat transfer enhancement in different geometries both numerically [11]–[13] and experimentally [12-14]. Jaramillo et al. [17] analyzed a parabolic trough collector integrating a twisted tape. They found that using the twisted tape improve the efficiency of the solar collector under conditions of low twisted ratios operating at low Reynolds numbers. Mwesigye et al. [18] studied the hydrothermal characteristics of a parabolic trough receiver numerically integrating with wall-detached twisted tape. They showed a higher optimal Reynolds number for a higher twist ratio and lower width ratios. Man et al. [19] performed an empirical study of a double-pipe heat exchanger in which the inner tube is equipped with alternation of clockwise and counterclockwise twisted tape compared with conventional twisted tape. They concluded that their proposed twisted tape shows a better thermal performance than the typical one. They employed the performance evaluation criterion (PEC) number to show the enhanced heat transfer versus increased pumping power and reported the highest value of 1.42 for this number in their experimental conditions. Lim et al. [20] also studied a double-pipe heat exchanger equipped with twisted tape inserts with different pitch ratios. They provided the predictions of heat transfer characteristics for various Reynolds numbers. Saylroy and Eiamsa-ard [21] embedded a square cut twisted-tape in a circular tube and numerically analyzed it. They reported the highest PEC number of 1.37 in their operating conditions. Later on, in another study, Saylroy and Eiamsa-ard [22] investigated the multi-channel twisted tapes and showed an enhancement of laminar convection heat transfer through applying such twisted tapes. Sundar et al. [23] studied and analyzed the thermal performance of a solar water heater using passive techniques of nanofluid and twisted tape. They concluded that at Re=13000, 21%

modification occurs in heat transfer for 0.3% nanofluid for the plain tube while it is enhanced by almost 50% using twisted tape. He et al. [24] employed cross hollow twisted tape inserts in a tube to empirically study its thermal characteristics. They showed that the PEC number ranges from 0.87 to 0.98 for Reynolds numbers varying from 5600 to 18000. Qi et al. [25] studied rotating and static built-in twisted tapes using nanofluid experimentally. They showed that using rotating twisted tape along with the nanofluid result in 101.6% enhancement in heat transfer. Ravi Kumar et al. [26] employed the effectiveness-number of transfer units (ε-NTU) method to assess a double-pipe U-bend integrating twisted tape showing effectiveness enhancement. Samruaisin et al. [27] investigated regularly-spaced quadruple twisted tape elements in a tube in the turbulent regime and found the maximum value of 1.27 for PEC number in the range of their operational conditions. Ruengpayungsak et al. [28] numerically investigated the heat transfer enhancement of a tube using centrally-perforated twisted tape inserts in both laminar and turbulent regimes and obtained the maximum value for PEC number to be approx. 8.92 and 1.33 for laminar and turbulent regimes, respectively. Hong et al. [29] carried out an empirical study of a spiral grooved tube equipped with twin overlapped twisted tapes in turbulent regime with Reynolds numbers of 8000 to 22000. Their results revealed an enhancement in both heat transfer and friction coefficient as the overlapped twisted ratio augments. Later, Hong et al. [30] employed overlapped multiple-twisted tapes in a similar experimental study. They showed lower and higher entropy generation due to heat transfer and friction resistance, respectively, for a higher tape number and a lower overlapped twisted ratio. Hasanpour et al. [31] investigated the hydrothermal characteristics of a corrugated tube heat exchanger inserting twisted tapes using the optimization method. They the maximum heat transfer at V-cut twisted tape model and the minimum pressure drop is achieved at perforated twisted tape model. Later on, a numerical study of a tri-lobbed tube equipped with twisted tapes performed by Hemmat Esfe et al. [32] in Reynolds numbers varying from 5000 to 20000. They

showed that the pitch ratio enhancement causes an increase in Nusselt number, friction factor and overall thermal performance. Rashidi et al. [33] studied nanofluid flow through a square duct fitted with transverse twisted-baffles. They presented lower entropy for a higher nanoparticles concentration and also for the case with baffles in the duct. They also reported the optimum geometries in terms of maximum heat transfer and minimum pressure drop.

Reviewing the literature in this field suggests that indeed, many attempts have been made in recent years to study different types of twisted tape inserts with different configurations and in various geometries. Besides, many parametric studies have been carried out to analyze the effect of various twisted tapes toward the optimal configurations. However, in nearly all the studies performed in this field so far, the twisted tapes were stationary and to the best of authors' knowledge, no study has been carried out to investigate the effect of using rotating twisted tapes examining the angular velocity and twisted tape pitch effects which the setup of rotating tube with twisted tape inserts first was conducted in the experimental study of Muralidhara Rao and Sastri [34]. Therefore, this study aims to numerically analyze the application of rotating twisted tapes for laminar convection heat transfer enhancement in a tube. Finally, the performance evaluation criterion is presented to evaluate the effectiveness of using rotating twisted tape at different pitch magnitudes.

2. Problem Definition

2.1 Geometrical Details

Fig. 1 shows the schematic of a tube equipped with a twisted tape. The height of the twisted tape, H, is 95% of the tube diameter (D=20 mm) and length (L= 400 mm) with the thickness, t = 0.4 mm and equivalent pitches of 400 mm. Besides, r and θ are the radial and tangential directions, respectively. Water enters the tube at the temperature of 300K and constant heat

flux is applied at the walls. The twisted tape is rotating inside the tube at three angular velocities of $\frac{V_{\text{inlet}}}{r}$ (i.e. RTT1), $\frac{2V_{\text{inlet}}}{r}$ (i.e. RTT2), and $\frac{3V_{\text{inlet}}}{r}$ (i.e. RTT3).

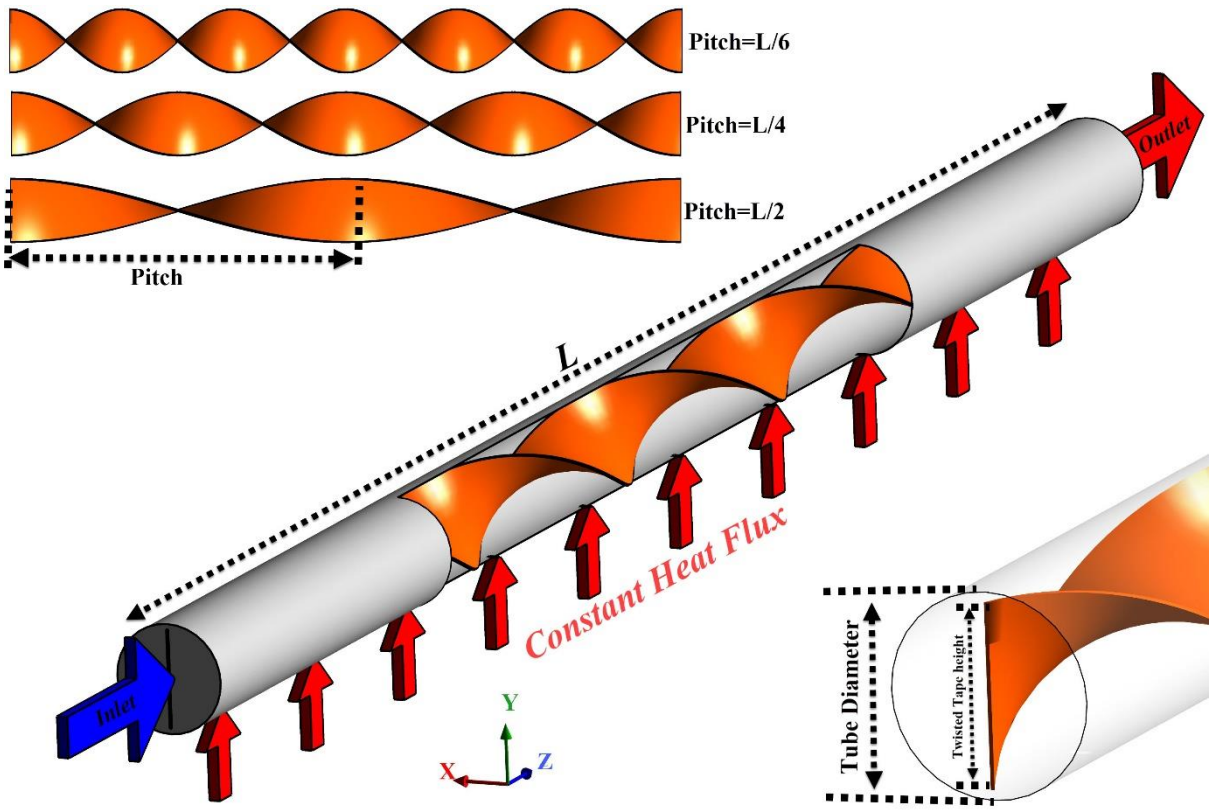

Fig. 1. A heat pipe integrated with twisted tape

2.2. Governing equations

This research investigated a steady laminar flow of incompressible water fluid neglecting the effects of radiation and viscosity losses. The governing equations are defined below.

$$\nabla . \left(\rho \vec{V}\right) = 0 \tag{1}$$

$$\nabla . \left(\rho \vec{V} \vec{V}\right) = -\nabla p + \mu \nabla^2 \vec{V} \tag{2}$$

$$\nabla . \left(\rho \vec{V} C_p T\right) = \nabla . \left(k \nabla T\right) \tag{3}$$

The local and average coefficient of heat transfer, as well as friction factor, are defined as:

$$f_{\text{avg}} = \left(-\frac{\Delta P}{l}\right) \frac{D}{1/2 \rho U^2} \tag{4}$$

$$h_x = \frac{q''}{T_w - T_b} \tag{5}$$

$$Nu_x = \frac{h_x D_h}{k} \tag{6}$$

$$Nu_{\text{avg}} = \frac{1}{l}\int_0^l Nu_x dx \tag{7}$$

where

$$D_h = \frac{4A}{P} \tag{8}$$

PEC number is defined by many authors [33-35] in the literature to evaluate the performance of the heat exchanger; however, since the motor power exists in this study, PEC number is defined based on the total energy consumption in this study as follow:

$$\text{PEC} = \frac{\text{Nu}/\text{Nu}_s}{(\dot{E}_c/\dot{E}_{c,s})^{1/3}} \tag{9}$$

In Eq. (9), subscript "s" belongs to PT and $\dot{E}_c$ represents the total energy consumption in the system including pumping power and motor power (as a motor is needed to drive the rotation of the twisted tape which is equal to zero in PT and STT cases). The energy consumption is therefore defined as follows:

$$\dot{E}_c = \dot{W}_{\text{p}} + \dot{W}_{\text{m}} \tag{10}$$

where

$$\dot{W}_{\text{p}} = \dot{V}\Delta p \tag{11}$$

$$\dot{W}_{\text{m}} = T\omega \tag{12}$$

$$\text{T} = \left(\int_{\text{s}} \left(\vec{\text{r}} \times (\bar{\bar{\tau}} \cdot \hat{\text{n}})\right)\text{ds}\right) \cdot \hat{\text{a}} \tag{13}$$

where ω is the angular velocity, T is the torque, S is the surface comprising all rotating parts, $\bar{\bar{\tau}}$ is the total stress tensor, $\hat{\text{n}}$ is a unit vector normal to the surface, $\vec{\text{r}}$ is the position vector and $\hat{\text{a}}$ is a unit vector parallel to the axis of rotation. In the CFD post-processing module, the torque is calculated from the above surface integral on the moving parts with respect to the axial

direction. Knowing the torque from the CFD post, it is possible to estimate the power consumption through multiplying it by the rotational speed [38].

2.3. Boundary conditions

At the tube inlet, constant velocity and temperature are considered while pressure outlet is employed at the outlet. The channel wall is exposed to a uniform heat flux of 5000 W/m^2 and the twisted tape rotates at three different angular velocities in which its outer walls are adiabatic. In fact, the rotating wall boundary condition is used in this study for simulating the rotating twisted tapes [39], [40].

3. Numerical Procedure

3.1. Code and Convergence

The commercial CFD code ANSYS FLUENT (version 18.0) is employed using the Coupled algorithm for the velocity–pressure coupling [41], [42]. Design Modeler and Ansys Meshing are used to generate the geometry and grid in this study, respectively. Moreover, the second-order upwind scheme is used for discretization of both momentum and energy equations. The convergence criteria are considered less than 10^{-6}, 10^{-6}, and 10^{-9}, respectively, for continuity, momentum, and energy equations, along with the observation of mass-weighted average magnitudes of velocity and temperature at the tube outlet.

3.2. Grid

Fig. 2 displays the mesh which is refined near the wall regions due to the presence of large velocity and temperature gradients. Grids with different numbers of elements are examined to ensure the grid independency. The average Nusselt number has been selected as the criteria to examine the grid independency. Table 2 presents the cases considered for mesh independence

analysis. Case 3 has eventually been chosen to conduct all the simulations, since using finer meshes lead to relative errors less than 1%.

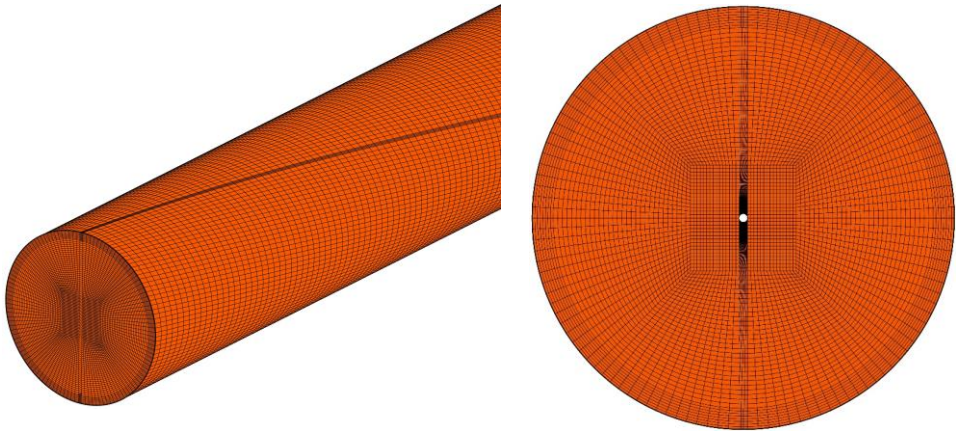

Fig. 2. The final mesh used in the present study.

Table 2. Grid independence analysis.

Case	Number of elements	Nusselt number	Error (%)
1	1,000,000	26.30	33.11
2	1,350,000	25.35	3.70
3	1,750,000	25.21	0.59
4	2,250,000	25.20	0.03

3.3. Experimental Validation

To verify the code, the average Nusselt number for different Reynolds numbers reported in the study of Sundar and Sharma [43] is considered as a comparison parameter. Sundar and Sharma empirically investigated the effects of twisted tape inserts with the thickness of 1mm and height to diameter ratio of 5 on fully-developed laminar convective heat transfer through a copper tube with 12 mm diameter exposing to a constant heat flux of 1000 W. As shown in Fig. 3, there is a good agreement between the experimental data and present numerical results.

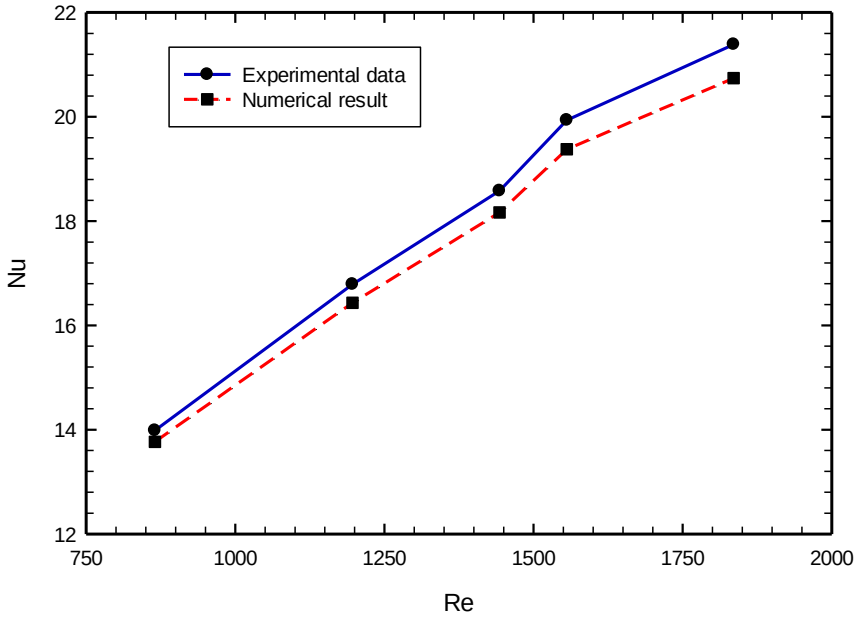

Fig. 3. Validation study against the data of Sundar and Sharma [43].

4. Results and Discussion

Numerical simulations are performed for a circular tube inserting stationary twisted tapes (STT) and rotating ones with three angular velocities (RTT1, RTT2, RTT3) at three pitches of L/6, L/4, L/2 and four Reynolds numbers of 250, 500, 750, 1000.

Fig. 4 displays the local Nusselt number along the tube length for plain tube and STT insert at different pitches and Reynolds number of 250. This figure shows that using STT insert and decreasing its pitch increases the local Nu significantly throughout the tube length. In fact, STTs generate a swirling/secondary flow, leading to an enhancement in flow mixing and thermal boundary layer disturbance, which in turn increases heat transfer. In other words, the twisted tape redirects the colder core fluid with the higher cooling capacity to the heated walls of the tube where cooling is required. Also, decreasing the twisted tape pitch intensifies such phenomenon resulting in higher local Nu and heat transfer.

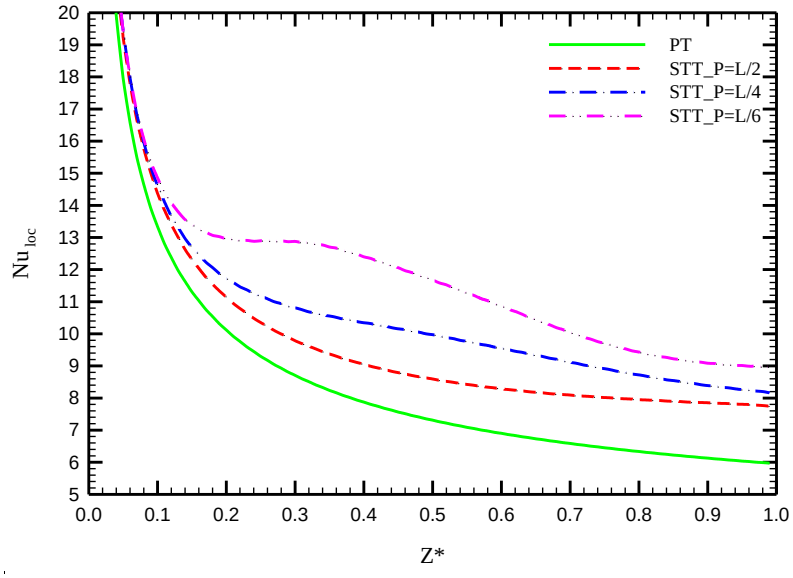

Fig. 4. Local Nu along the tube length for plain tube and STTs with three pitches (L/2, L/4, L/6) at Re = 250.

To clarify the reason for heat transfer enhancement by twisted tape pitch reduction in Fig. 4, Fig. 5 presents streamlines colored by velocity magnitude for plain tube and STT at various pitches. The swirl flow generation in the presence of STTs can clearly be seen in this figure. It is evident that as the twisted tape pitch decreases, the mixing flow strengthens resulting in stronger secondary flow, consequently, higher heat dissipation from the heated wall is achieved. Besides, looking at the generated swirl flow patterns shows that at lower twisted tape pitch values, more radial velocity is obtained, implying a better flow mixing and secondary flow and as a result more efficient cooling process.

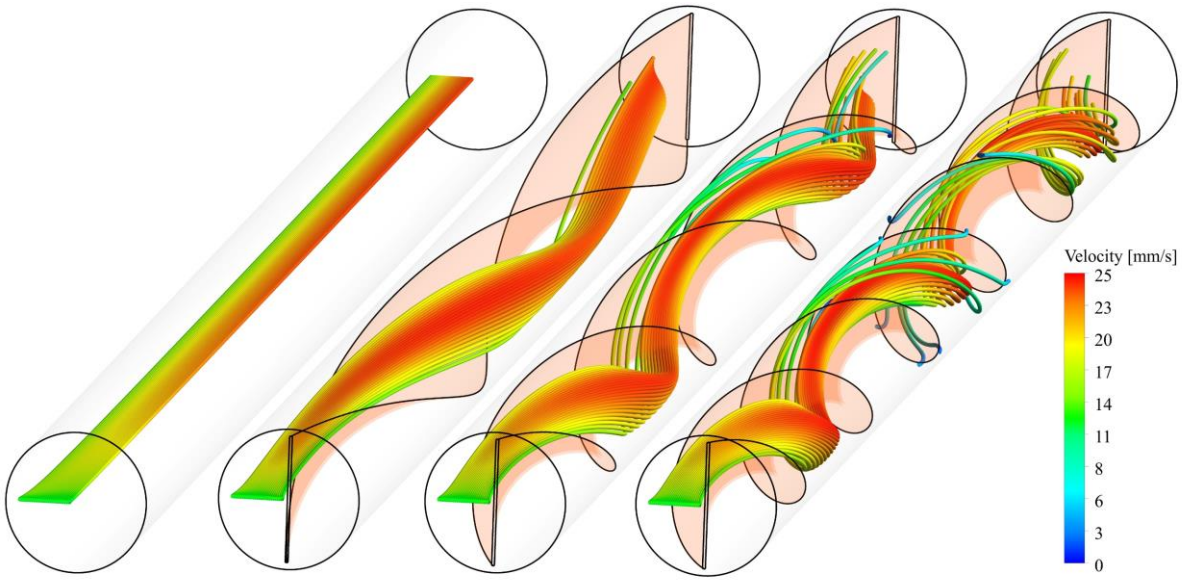

PT P=L/2 P=L/4 P=L/6

Fig. 5. Streamlines colored by velocity magnitude for cases of the plain tube and STT with three pitches of L/2, L/4, L/6 at $Re = 250$.

The effect of twisted tape pitch on the cooling of the heated wall at $Re = 250$ is shown in Fig. 6. The temperature distribution on the heated wall indicates the cooling capacity and the secondary flow intensity. In the plain tube, the temperature continuously increases through the tube length as the fluid flows showing the thermal boundary layer development. Inserting the twisted tape has modified the temperature distribution and has made it more uniform with some hot spots following the twisted tape pitch reduction. As the twisted tape pitch decreases the temperature distribution gets more uniform and also the outlet temperature decreases indicating the better cooling performance of the system.

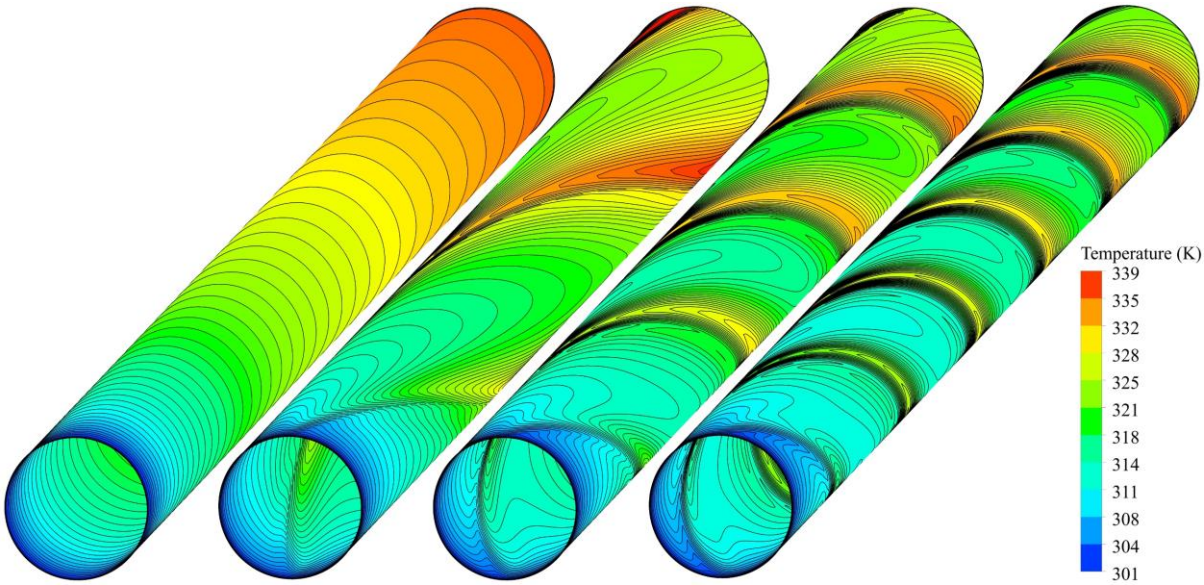

PT P=L/2 P=L/4 P=L/6

Fig. 6. Temperature contours on the heated wall for cases of the plain tube and STT with three pitches of L/2, L/4, L/6 at $Re = 250$.

Fig. 7 displays the cross-sectional temperature contours, at five surfaces with the distance of L/4 from each other, for plain tube and STT with different pitch values at $Re = 250$. The plain tube cross-sectional temperature contours show the normal development of the thermal boundary layer along the tube length followed by a significant drop in heat transfer. Inserting the twisted tape results in a thinner thermal boundary layer due to the disturbance of this layer via the STT resulting in improved heat transfer rate between the heated wall and the fluid across the channel; however, there are still some hotspots in the temperature contours along the tube length affecting the displayed hotspots on the temperature distribution of the heated wall in Fig. 6. Moreover, the redirection of the colder core fluid to the vicinity of the heated wall is visible by using STT leading to an enhanced secondary flow and heat dissipation from the heated wall. Both phenomena, including thinner thermal boundary layer through the tube length and improved flow mixing by redirecting the colder core flow to the heated wall, are observed as the twisted tape pitch reduces, implying a better cooling process. Besides, some

local hotspots along the perimeter are visible in this figure which would cause local thermal stress and would be harmful in practical usages. As a result, in such cases, more manufacturing considerations are required.

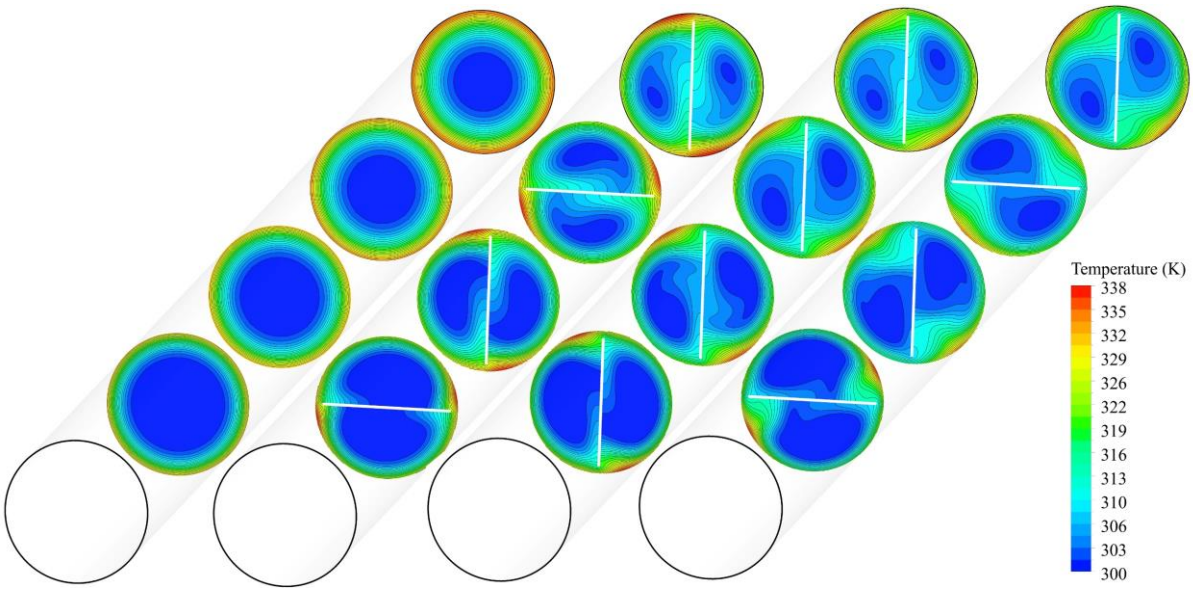

PT P=L/2 P=L/4 P=L/6

Fig. 7. temperature contours for plain tube and STT with three pitches of L/2, L/4, L/6 at $Re = 250$ at different cross-sections.

Since the cross-sectional velocity of the fluid along the channel length indicates the secondary flow intensity, Fig. 8 is provided in which the cross-sectional velocity contours and vectors through the tube for plain tube and STT with different pitches at $Re = 250$ are shown. The plain tube velocity contours represent the expected development of the hydrodynamic boundary layer and velocity distribution through the channel showing the maximum velocity in the core with the most capacity of cooling resulting in ineffective cooling. On the other hand, inserting STTs has transferred the colder core fluid velocity to the heated wall vicinity resulting in better heat transfer between the wall and fluid. This has been strengthened as the twisted tape pitch has decreased which has led to a higher heat transfer rate.

To quantify the heat transfer and fluid flow characteristics of the so far presented cases, figures 9 and 10 are provided to show the variations of average Nu and f with respect to the Re for the plain tube and STT with three various pitches. Fig. 9 illustrates that increasing Re increases Nu and the heat transfer rate due to the better advection effect of the fluid and higher fluid momentum near the heated wall. This can be also explained using Fig. 11 which indicates a thinner thermal boundary layer. Moreover, improved distribution of the colder core fluid around the heated wall at higher Reynolds numbers in a cross-sectional surface in the middle of the tube length is visible in this figure. The improvement of the cooling performance by applying STT and decreasing its pitch can also be observed in Fig. 11 such that compared to the case of the plain tube, using SST with the pitch of L/2, L/4, L/6 respectively increases the average Nu by approx. 15%, 24%, 37% for Re of 250; 17%, 45%, 68% for Re of 500; 19%, 56%, 75% for Re of 750; 23%, 61%, 79% for Re of 1000.

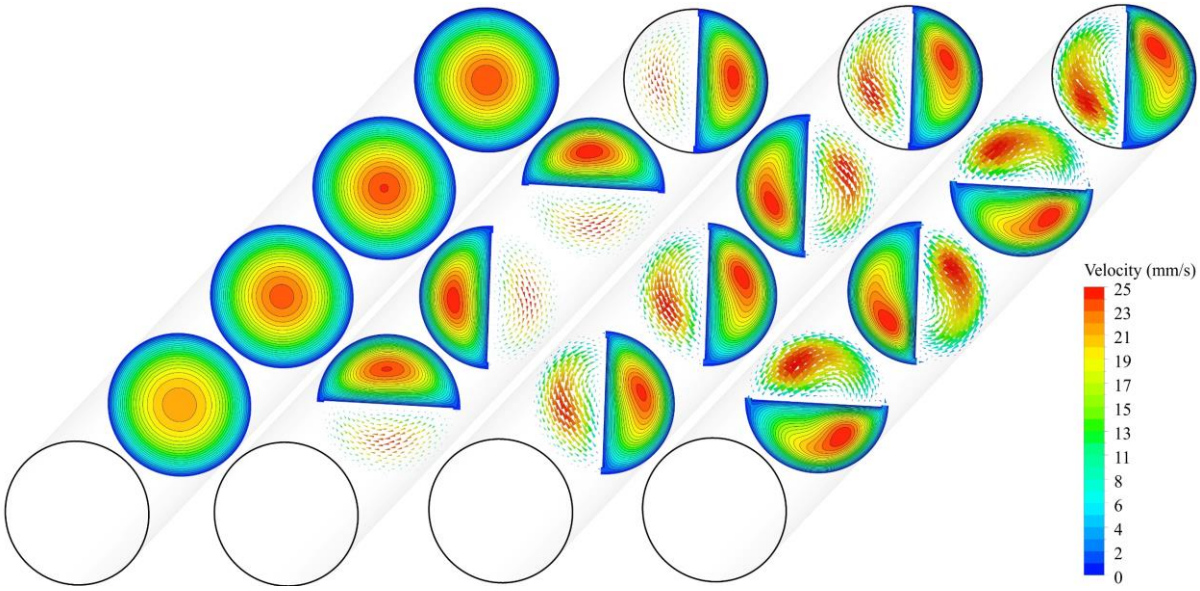

Fig. 8. Cross-sectional velocity contours and vectors for cases of the plain tube and STT with three pitches of L/2, L/4, L/6 at $Re = 250$.

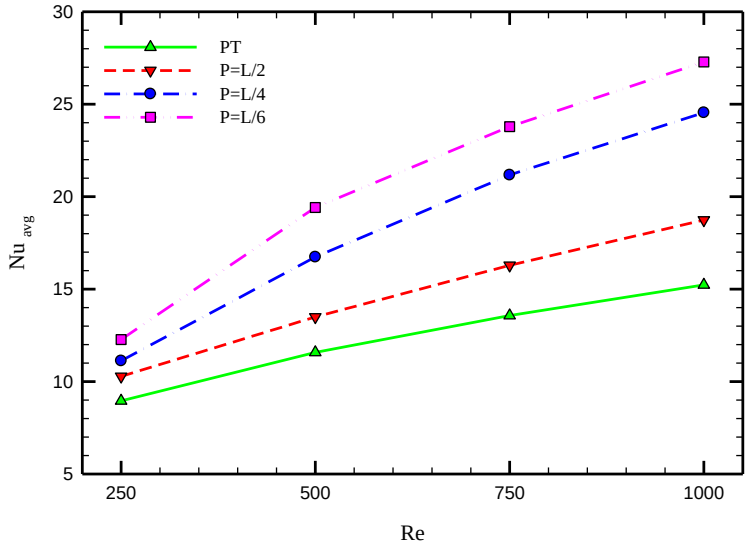

Fig. 9. Average Nu for the plain tube and STT at various Reynolds numbers and twisted tape pitch values.

Fig. 10 demonstrates that inserting STT results in higher values for f due to the added surface area of the twisted tape for fluid flow and also the flow blockage created by the tape inserted in the tube. The same effect can be seen when decreasing the twisted tape pitch. This figure also reveals that Re is inversely proportional to f. This can be explained using equation (18) which includes U^2 in the denominator of f correlation. This is also can be explained using Fig. 11 which indicates more flow mixing and intense secondary flow in a cross-sectional surface in the middle of the tube length.

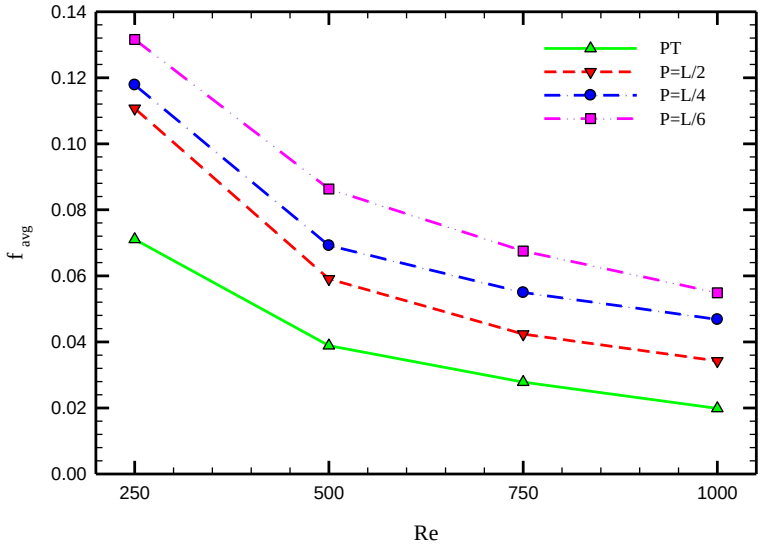

Fig. 10. Average f for different cases of plain tube and STT at various Reynolds numbers twisted tape pitch values.

For the remainder of this section, the heat transfer and fluid flow characteristics of the cases studied so far will be investigated by applying rotating twisted tapes with three angular velocities (RTT1, RTT2 and RTT3).

Fig. 12 displays the local Nu along the tube length for the cases of STT, RTT1, RTT2, and RTT3 with three twisted tape pitches at Re=250. This figure reveals that at all twisted tape pitches as the twisted tape starts to rotate the local Nu increases through the tube due to the fact that applying RTT causes better mixing flow, more intense secondary flow and higher disturbance of the thermal boundary layer and as a result, enhanced cooling performance is achieved. On the other hand, increasing the twisted tape angular velocity at the three twisted tape pitches from RTT1 to RTT3 shows a slight enhancement in local Nu through the channel.

To better quantify the overall heat transfer in the proposed cases, Fig. 13 is provided to represent the variations of average Nu with the plain tube and three pitches of twisted tape for cases of STT, RTT1, RTT2, and RTT3 at $Re = 250$. This figure highlights the differences

between the STT and RTT cases variations with twisted tape pitch reduction. This figure reveals that as the twisted tape starts to rotate, decreasing its pitch does not have any significant effects on the heat transfer rate. Furthermore, increasing the angular velocity from RTT1 to RTT2 leads to a notable heat transfer enhancement, while further increasing the angular velocity from RTT2 to RTT3, has a much small impact on heat transfer. The reason is that disturbing and thinning the thermal boundary layer from RTT1 to RTT2 is noticeable; however, the thermal boundary layer is thinned enough as using RTT3 over RTT2 is less effective. This implies that raising the angular velocity any further beyond RTT2 is unlikely to bring any useful benefits and in fact may result in the waste of energy. In this figure, the average Nu increases by about 65.9%, 63.6%, 55.1%, and 39.0% in the cases of STT, RTT1, RTT2, and RTT3, respectively, for Re of 1000 and the twisted tape pitch value of L/6. This potential waste of energy is more noticeable when considering f variations in different cases in Fig. 14, in which higher f values are obtained at higher twisted tape angular velocities. The same trend between the Nu and f is observed by decreasing the twisted tape pitch in RTT cases such that the f variations with twisted tape pitch reduction in RTT cases is insignificant.

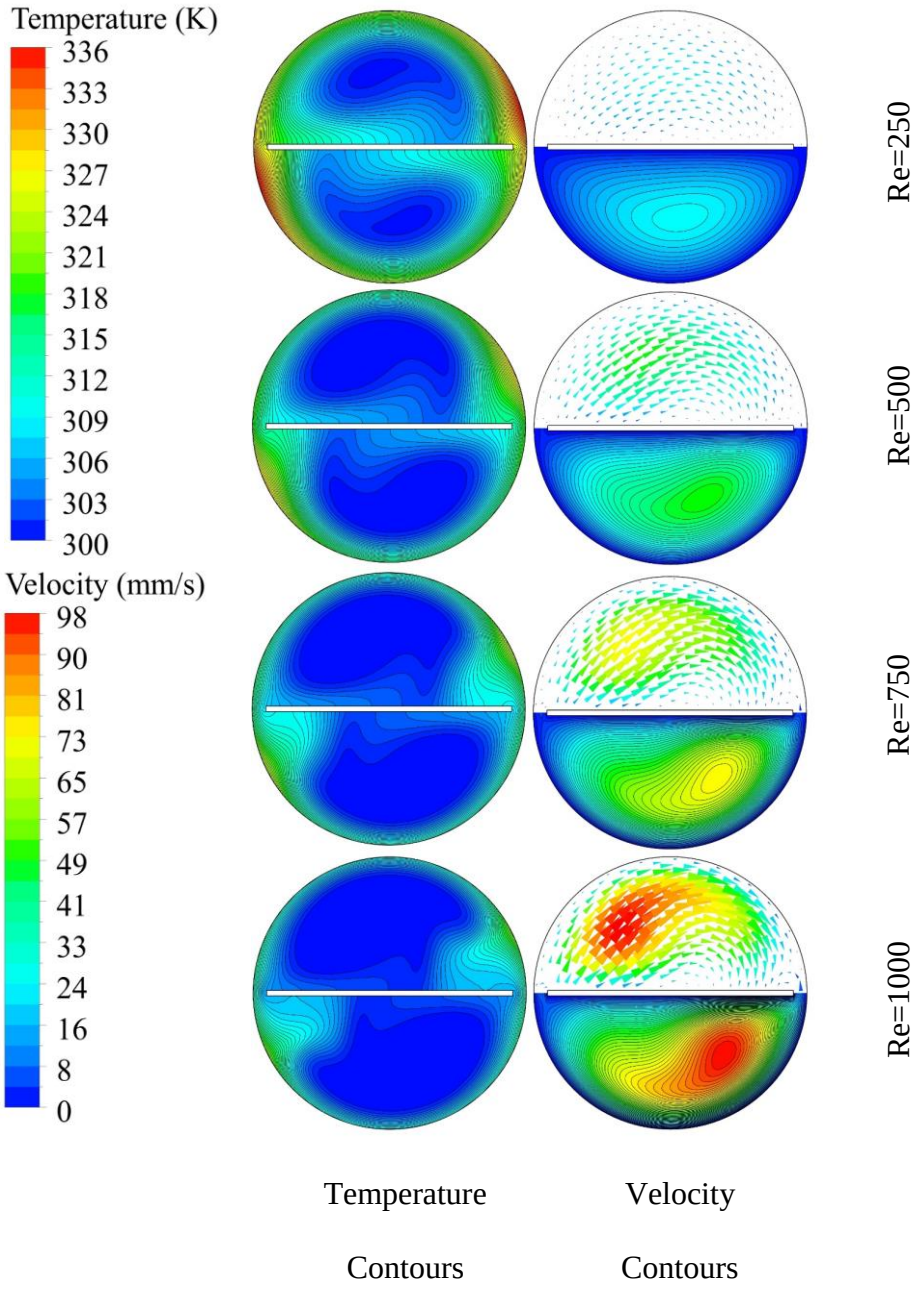

Fig. 11. Temperature, velocity contours and vector on a cross-sectional plane located at L=0.3 in the STT case at P= L/2 and Re= 250, 500, 750, 1000.

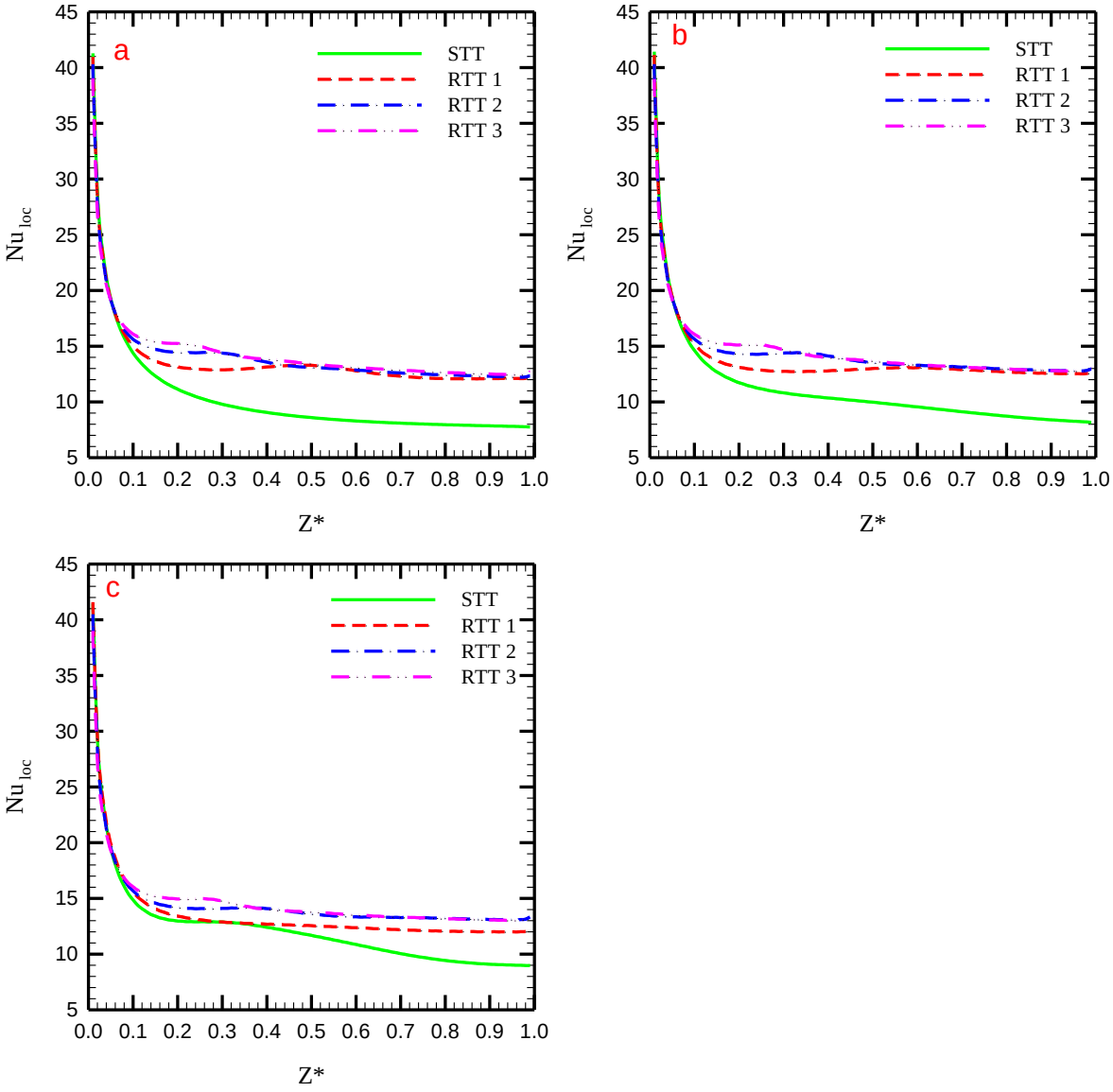

Fig. 12. Local Nu through the tube length for three twisted tape angular velocities, at Re=250 and (a) P= L/2, (b) P= L/4, and (c) P= L/6.

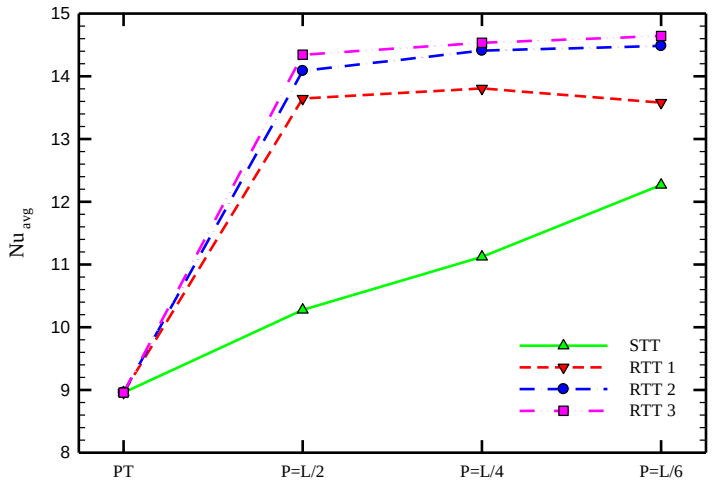

Fig. 13. Average Nu for different cases of STT, RTT1, RTT2, and RTT3 at various pitch values.

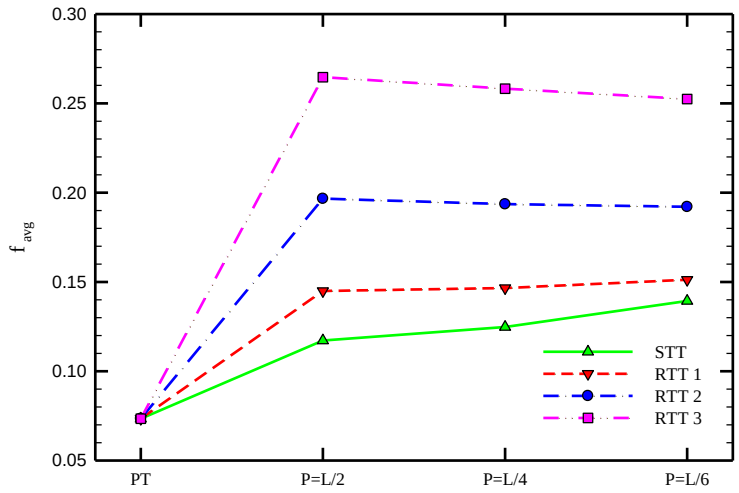

Fig. 14. Average f for different cases of STT, RTT1, RTT2, and RTT3 at various pitch values.

Fig. 15 illustrates the temperature and velocity contours and vectors at different cross-sections for the cases of STT, RTT1, RTT2, and RTT3 at twisted tape pitch of L/2 and $Re = 250$. The temperature contours indicate that the thermal boundary layer of STT case is much thicker than those of RTT cases, also a better redirection of the colder core fluid to the heated wall vicinity is observable in RTT cases proving the heat transfer improvement in RTT cases. Besides, the

slight difference in cross-sectional temperature contours of RTT2 and RTT3 cases in their thermal boundary layer and colder core fluid distribution implies a slight difference in heat transfer of these cases shown in Fig. 13 quantitatively. The velocity contours and vectors show the higher secondary flow intensity at RTT cases and also better mixing flow at higher angular velocities.

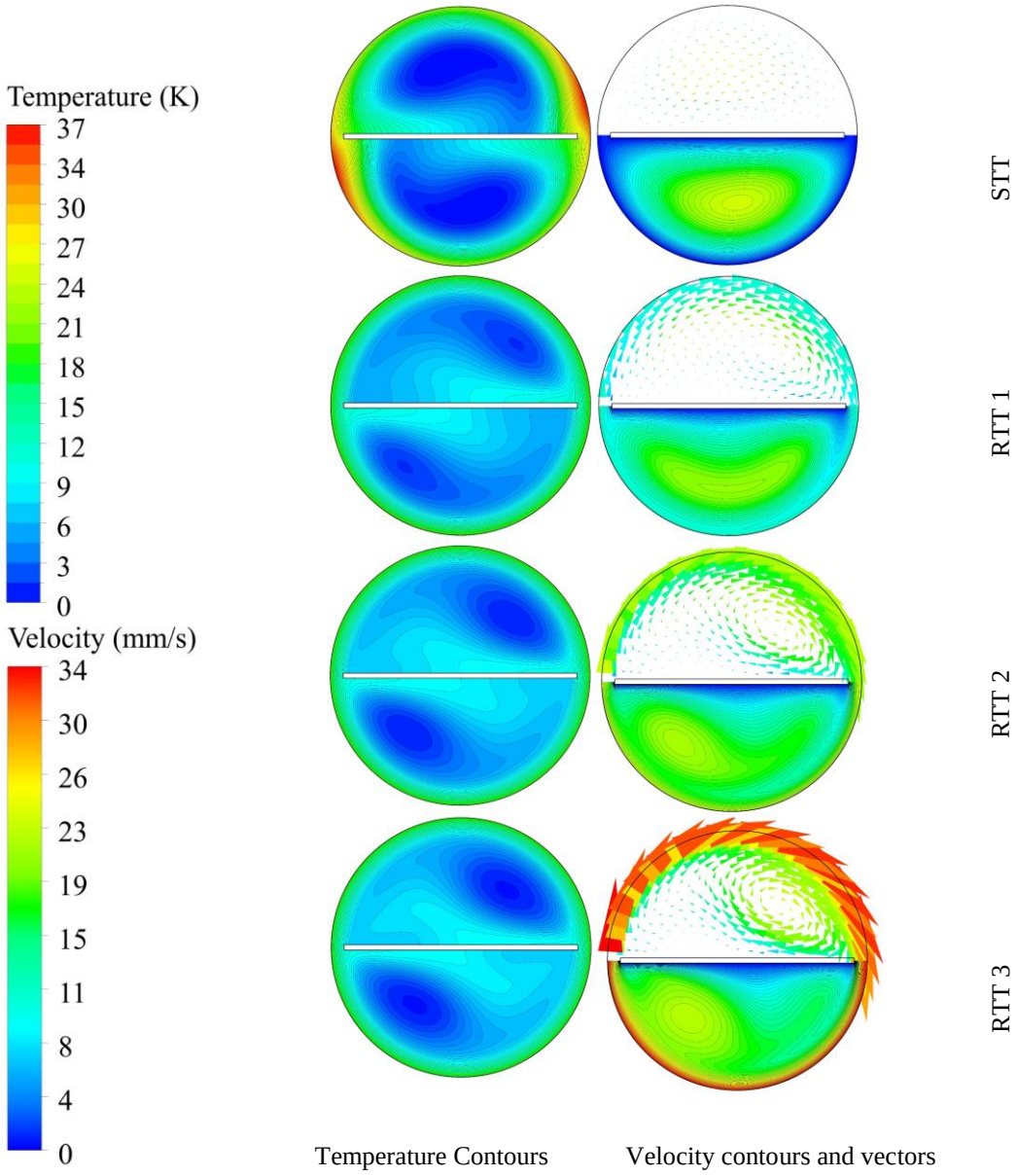

Fig. 15. Temperature, velocity contours and vectors on a cross-sectional plane located at L=0.3 in the cases of STT, RTT1, RTT2, and RTT3 at P= L/2 and Re= 250.

Fig. 16 depicts the streamlines colored by velocity magnitude for the cases of STT, RTT1, RTT2 and RTT3 at the twisted tape pitch of L/2 and $Re = 250$. The figure shows that STT redirects the flow path and creates a smooth secondary flow in the tube. However, as the twisted tape starts to rotate, the flow experiences a strong swirling effect in which swirl flow patterns are visible in the streamlines. Looking at the first pitch of the twisted tape (from inlet to the half-length of the tube) reveals that as the angular velocity increases from RTT1 to RTT3, the number of swirling flow vortices increases from one to three. These large swirling vortices result in more effective mixing flow that the colder core fluid is redirected more effectively towards the heated wall in comparison with the STT case. Moreover, higher velocity magnitudes are visible at the heated wall vicinity as the twisted tape angular velocity augments. This can be attributed to the streamlines color at the wider section of the swirl flow patterns varying from green to red by enhancing the angular velocity from RTT1 to RTT3.

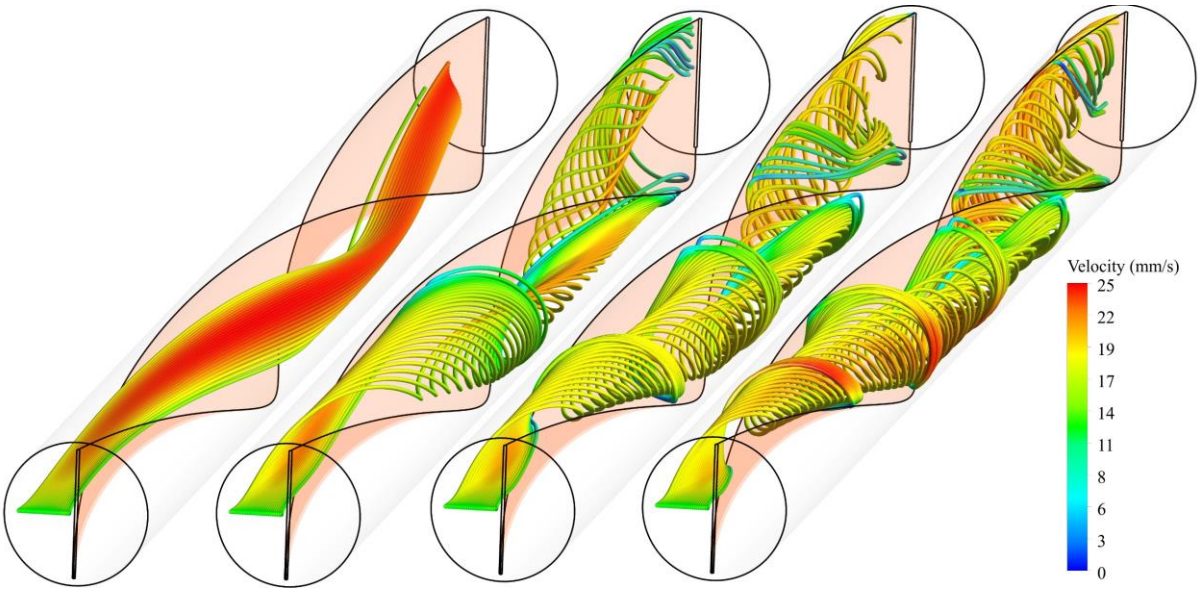

Fig. 16. Streamlines colored by velocity magnitude for cases of STT, RTT1, RTT2, and RTT3 at P= L/2 and Re= 250.

Fig. 17 displays the pumping power and energy consumption of the system in all captured configurations. As displayed in Fig. 17 (a), a higher Reynolds number causes higher pumping power due to the generation of more intense mixing and secondary flow and also higher contact area between the fluid and solid twisted tapes. In addition, this figure reveals that decreasing the pitch of the twisted tape increases the pumping power in case of the stationary twisted tape as a result of stronger secondary flow and the higher contact area between the fluid and solid. This enhancement in pumping power by pitch reduction reduces as the twisted tape starts to rotate, such that there is a subtle change in the pumping power for RTT3. The reason is attributed to an intense disturbance in the viscose boundary layer in RTTs, prohibiting the growth of the boundary layer through the channel. This phenomenon is further intensified by increasing the twisted tape angular velocity, such that the twisted tapes with different pitch values in RTT3 case have almost equivalent pumping power values. The highest pumping power values correspond to the STT cases followed by RTT1, RTT2 and RTT3 cases. Figure 17(b) shows the electric motor power consumption for rotating twisted tape cases. As seen in this figure, increasing the Reynolds number and twisted tape angular velocity is accompanied by an increase in the electric motor consumption, while a decrease in the pitch of the twisted tape reduces the electric power required to rotate the twisted tape. Figure 17(c) shows the total energy consumption of the considered configurations at different Reynolds numbers and various pitch distance of the twisted tapes. It is evident that higher Reynolds number and angular velocity enhances the total energy consumption of the system. The results of this figure suggest that a decrease in the pitch of twisted tape increases the total energy consumption of STT. Moving from STT to RTT1 results in reducing the rate of increase in the energy consumption. Further increase in the angular velocity (i.e. RTT2 and RTT3) is associated with a reduction in the energy consumption due to the domination of lower motor power consumption to the higher pumping power requirement in these cases.

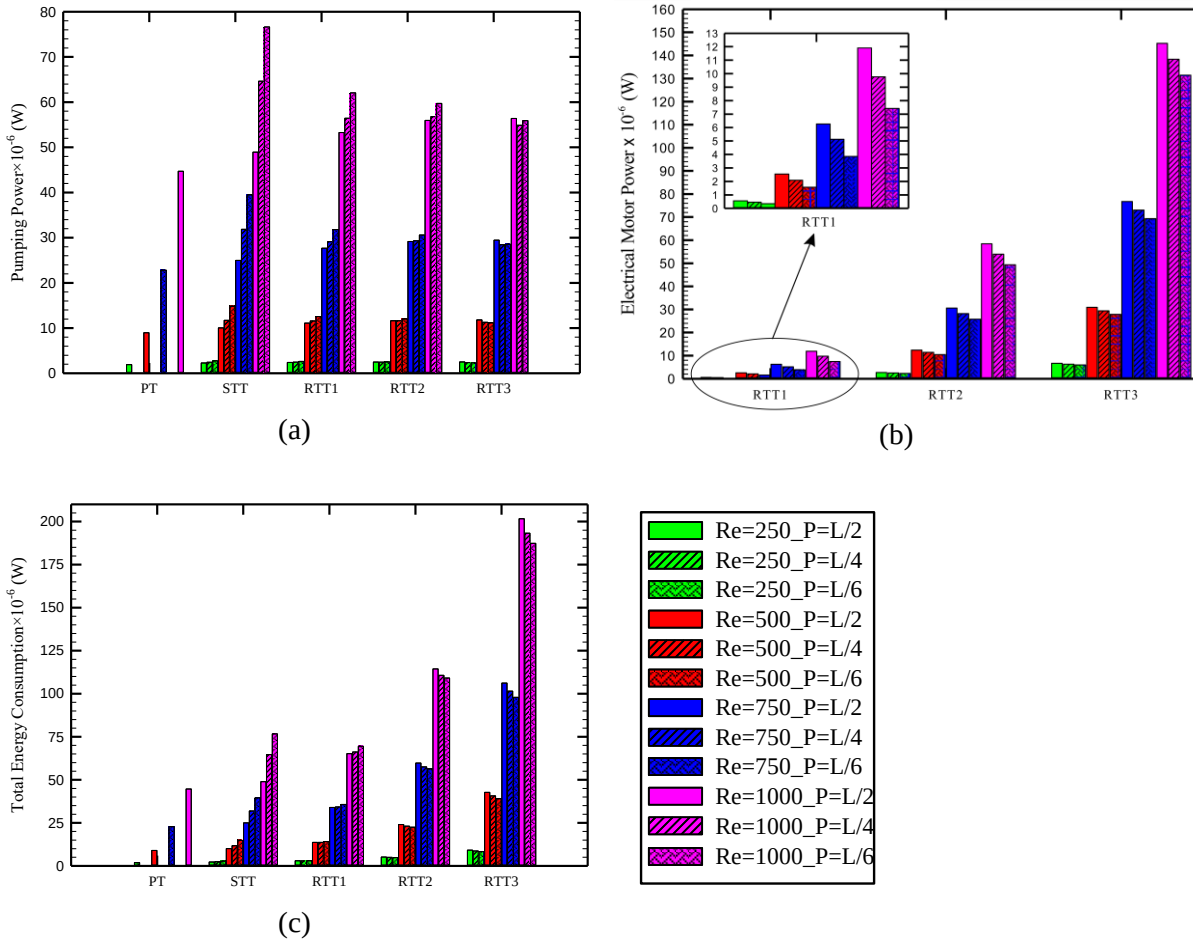

Fig. 17. (a) Pumping power, (b) electric motor power and (c) total energy consumption.

The discussions presented above showed the enhancement of both heat transfer (as a desirable outcome) and energy consumption (as an undesirable outcome) in both stationary and rotating twisted tapes as well as lower twisted tape pitches. Hence, there must be a trade-off between the benefits of using STT and RTTs in lower pitches in heat transfer enhancement, and their side effects in requiring more pumping and motor powers. To evaluate this issue, the dimensionless number of PEC determined in Eq. (9) is examined here. It is worth noting that the PEC number represents the practical use of enhancement devices in the viewpoint of energy-saving potential in which higher PEC values imply superior energy saving. Also, the unit value for PEC represents the plain tube based on its definition.

Fig. 18 shows the PEC number for all captured configurations. At Re=250 and all three twisted tape pitches, applying RTT1 increases the PEC number; however, enhancing the angular

velocity from RTT1 to RTT2/RTT3 leads to a reduction in the PEC number. On the other hand, in the higher Reynolds numbers (500, 750, 1000), the PEC number reduces as the twisted tape starts to rotate in almost all cases. Consequently, applying the RTT instead of the STT is only practical and beneficial at lower Reynolds numbers, in terms of energy consumption. Overall, by comparing the PEC number for all cases, it is found that the highest PEC number (PEC=1.50) is found for the case of STT at Re=1000 and the twisted tape pitch value of L/6.

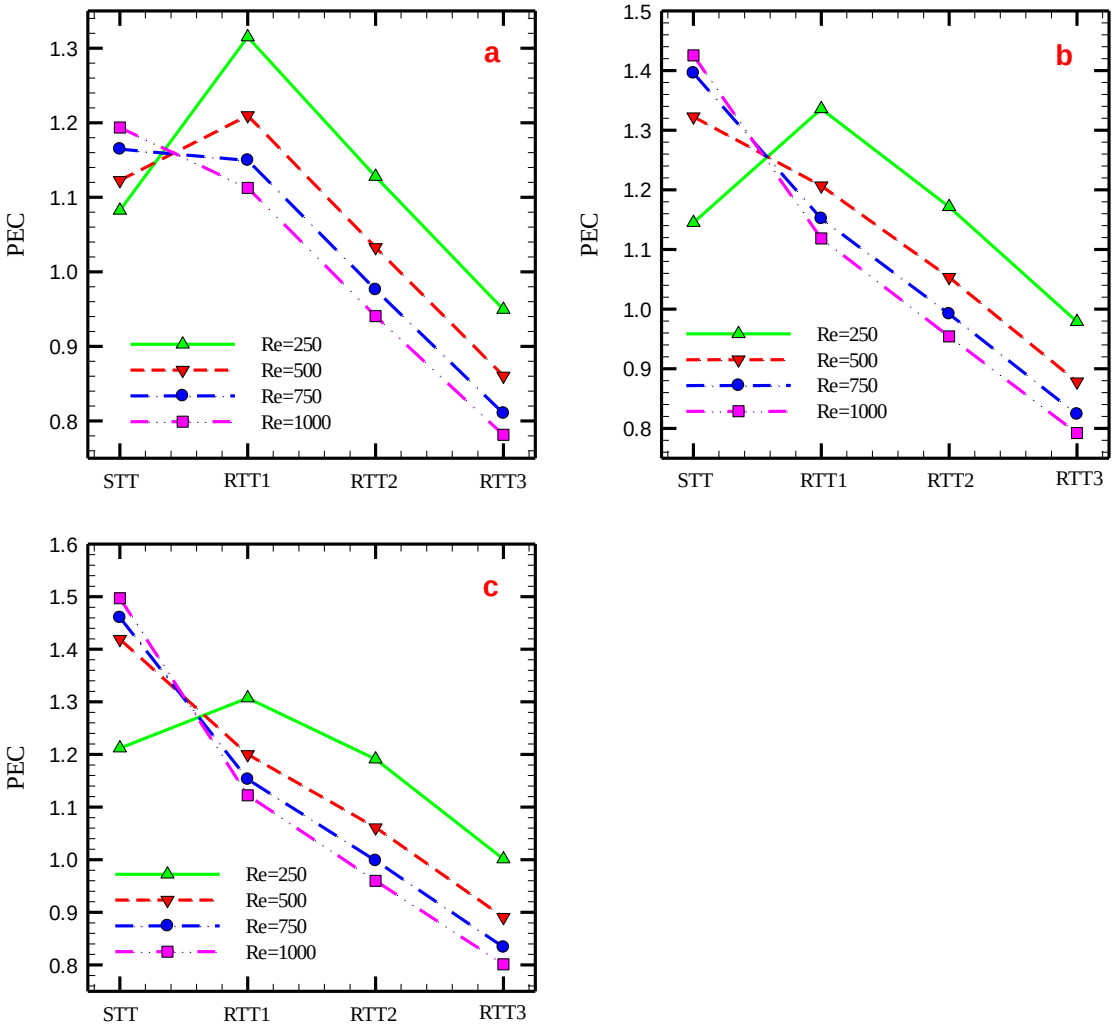

Fig 18. Variations of PEC number with three twisted tape angular velocities, at Re=250 and (a) P= L/2, (b) P= L/4, and (c) P= L/6.

5. Conclusion

In this study, a CFD-based parametric study was conducted to investigate the laminar convective heat transfer and fluid flow characteristics in a plain tube equipped with stationary and rotating twisted tapes with three angular velocities (RTT1, RTT2, RTT3) and three twisted tape pitches (L/2, L/4, L/6) at four Reynolds numbers (250, 500, 750, 1000). The main conclusions to draw from this work are as follows:

- Using twisted tape insert increases heat transfer, friction coefficient, energy consumption (including pumping power and motor power to drive the rotating twisted tape) and higher enhancement obtains as the twisted tape starts to rotate and the twisted tape pitch reduces.
- As the twisted tape starts to rotate, decreasing its pitch has no significant effect on the heat transfer rate, consequently, raising the angular velocity beyond a certain point (e.g. RTT2 in this case) is unlikely to bring any useful benefits and in fact may result in the waste of energy.
- Using SST with the pitch of L/2, L/4, L/6 respectively increases the average Nu by approx. 15%, 24%, 37% for Re of 250; 17%, 45%, 68% for Re of 500; 19%, 56%, 75% for Re of 750; 23%, 61%, 79% for Re of 1000. Also the average Nu increases by about 65.9%, 63.6%, 55.1%, and 39.0% in the cases of STT, RTT1, RTT2, and RTT3, respectively, for Re of 1000 and twisted tape pitch of L/6.
- From energy consumption viewpoint, applying rotating twisted tape instead of stationary twisted tape is only feasible and beneficial at lower Reynolds numbers.
- The present parametric study the highest dimensionless heat transfer to energy consumption ratio (represented through the PEC number) is found for the case of stationary twisted tapes at the Reynolds number of 1000 and the twisted tape pitch of L/6 which is equal to 1.50.

Author contributions:

Hossein Arasteh: Methodology, Software, Validation, Formal analysis, Investigation, Writing - Original Draft **Alireza Rahbari:** Conceptualization, Formal analysis, Writing - Review & Editing, Supervision **Ramin Mashayekhi:** Software, Validation, Formal analysis, Investigation **Amir Keshmiri:** Conceptualization, Writing - Review & Editing, Supervision **Roohollah Babaei Mahani:** Software, Writing - Review & Editing **Pouyan Talebizadehsardari:** Conceptualization, Formal anlysis, Writing - Review & Editing, Supervision

References

[1] A. K. Raj, M. Srinivas, and S. Jayaraj, "CFD modeling of macro-encapsulated latent heat storage system used for solar heating applications," *Int. J. Therm. Sci.*, vol. 139, pp. 88–104, 2019, doi: https://doi.org/10.1016/j.ijthermalsci.2019.02.010.

[2] P. Carrère and M. Prat, "Impact of non-uniform wettability in the condensation and condensation-liquid water intrusion regimes in the cathode gas diffusion layer of proton exchange membrane fuel cell," *Int. J. Therm. Sci.*, vol. 145, p. 106045, 2019, doi: https://doi.org/10.1016/j.ijthermalsci.2019.106045.

[3] J.-Y. Park, H.-W. Dong, H.-J. Cho, and J.-W. Jeong, "Energy benefit of a cascade liquid desiccant dehumidification in a desiccant and evaporative cooling-assisted building air-conditioning system," *Appl. Therm. Eng.*, vol. 147, pp. 291–301, 2019.

[4] D. T. Crane and L. E. Bell, "Maximum temperature difference in a single-stage thermoelectric device through distributed transport properties," *Int. J. Therm. Sci.*, vol. 154, p. 106404, 2020, doi: https://doi.org/10.1016/j.ijthermalsci.2020.106404.

[5] Y. Yan, Z. He, G. Wu, L. Zhang, Z. Yang, and L. Li, "Influence of hydrogels embedding positions on automatic adaptive cooling of hot spot in fractal microchannel

heat sink," *Int. J. Therm. Sci.*, vol. 155, p. 106428, 2020, doi: https://doi.org/10.1016/j.ijthermalsci.2020.106428.

[6] S. B. Ahangar, V. Konduru, J. S. Allen, N. Miljkovic, S. H. Lee, and C. K. Choi, "Development of automated angle-scanning, high-speed surface plasmon resonance imaging and SPRi visualization for the study of dropwise condensation," *Exp. Fluids*, vol. 61, no. 1, p. 12, 2020.

[7] S. B. Ahangar, K. Bellur, E. Medici, K. Tajiri, J. S. Allen, and C. K. Choi, "Optical properties and swelling of thin film perfluorinated sulfonic-acid ionomer," *ECS Trans.*, vol. 92, no. 8, p. 197, 2019.

[8] M.-H. Sun, G.-B. Wang, and X.-R. Zhang, "Rayleigh-Bénard convection of non-Newtonian nanofluids considering Brownian motion and thermophoresis," *Int. J. Therm. Sci.*, vol. 139, pp. 312–325, 2019, doi: https://doi.org/10.1016/j.ijthermalsci.2019.02.007.

[9] V. Singh, D. Haridas, and A. Srivastava, "Experimental study of heat transfer performance of compact wavy channel with nanofluids as the coolant medium: Real time non-intrusive measurements," *Int. J. Therm. Sci.*, vol. 145, p. 105993, 2019, doi: https://doi.org/10.1016/j.ijthermalsci.2019.105993.

[10] E. Abu-Nada, "Dissipative particle dynamics investigation of heat transfer mechanisms in Al2O3-water nanofluid," *Int. J. Therm. Sci.*, vol. 123, pp. 58–72, 2018, doi: https://doi.org/10.1016/j.ijthermalsci.2017.09.005.

[11] D. Yang, T. S. Khan, E. Al-Hajri, Z. H. Ayub, and A. H. Ayub, "Geometric optimization of shell and tube heat exchanger with interstitial twisted tapes outside the tubes applying CFD techniques," *Appl. Therm. Eng.*, vol. 152, pp. 559–572, 2019.

[12] A. Karimi, A. A. A. A. Al-Rashed, M. Afrand, O. Mahian, S. Wongwises, and A. Shahsavar, "The effects of tape insert material on the flow and heat transfer in a

nanofluid-based double tube heat exchanger: Two-phase mixture model," *Int. J. Mech. Sci.*, vol. 156, pp. 397–409, 2019, doi: https://doi.org/10.1016/j.ijmecsci.2019.04.009.

[13] M. Bahiraei, N. Mazaheri, and S. M. Hassanzamani, "Efficacy of a new graphene–platinum nanofluid in tubes fitted with single and twin twisted tapes regarding counter and co-swirling flows for efficient use of energy," *Int. J. Mech. Sci.*, vol. 150, pp. 290–303, 2019, doi: https://doi.org/10.1016/j.ijmecsci.2018.10.036.

[14] M. M. K. Bhuiya, M. M. Roshid, M. M. M. Talukder, M. G. Rasul, and P. Das, "Influence of perforated triple twisted tape on thermal performance characteristics of a tube heat exchanger," *Appl. Therm. Eng.*, vol. 167, p. 114769, 2020.

[15] S. Eiamsa-ard and K. Wongcharee, "Convective heat transfer enhancement using Ag-water nanofluid in a micro-fin tube combined with non-uniform twisted tape," *Int. J. Mech. Sci.*, vol. 146, pp. 337–354, 2018.

[16] B. Sajadi, M. Soleimani, M. A. Akhavan-Behabadi, and E. Hadadi, "The effect of twisted tape inserts on heat transfer and pressure drop of R1234yf condensation flow: An experimental study," *Int. J. Heat Mass Transf.*, vol. 146, p. 118890, 2020, doi: https://doi.org/10.1016/j.ijheatmasstransfer.2019.118890.

[17] O. A. Jaramillo, M. Borunda, K. M. Velazquez-Lucho, and M. Robles, "Parabolic trough solar collector for low enthalpy processes: An analysis of the efficiency enhancement by using twisted tape inserts," *Renew. energy*, vol. 93, pp. 125–141, 2016.

[18] A. Mwesigye, T. Bello-Ochende, and J. P. Meyer, "Heat transfer and entropy generation in a parabolic trough receiver with wall-detached twisted tape inserts," *Int. J. Therm. Sci.*, vol. 99, pp. 238–257, 2016.

[19] C. Man, X. Lv, J. Hu, P. Sun, and Y. Tang, "Experimental study on effect of heat transfer enhancement for single-phase forced convective flow with twisted tape

inserts," *Int. J. Heat Mass Transf.*, vol. 106, pp. 877–883, 2017.

[20] K. Y. Lim, Y. M. Hung, and B. T. Tan, "Performance evaluation of twisted-tape insert induced swirl flow in a laminar thermally developing heat exchanger," *Appl. Therm. Eng.*, vol. 121, pp. 652–661, 2017.

[21] A. Saysroy and S. Eiamsa-ard, "Periodically fully-developed heat and fluid flow behaviors in a turbulent tube flow with square-cut twisted tape inserts," *Appl. Therm. Eng.*, vol. 112, pp. 895–910, 2017.

[22] A. Saysroy and S. Eiamsa-Ard, "Enhancing convective heat transfer in laminar and turbulent flow regions using multi-channel twisted tape inserts," *Int. J. Therm. Sci.*, vol. 121, pp. 55–74, 2017.

[23] L. S. Sundar, M. K. Singh, V. Punnaiah, and A. C. M. Sousa, "Experimental investigation of Al2O3/water nanofluids on the effectiveness of solar flat-plate collectors with and without twisted tape inserts," *Renew. energy*, vol. 119, pp. 820–833, 2018.

[24] Y. He, L. Liu, P. Li, and L. Ma, "Experimental study on heat transfer enhancement characteristics of tube with cross hollow twisted tape inserts," *Appl. Therm. Eng.*, vol. 131, pp. 743–749, 2018.

[25] C. Qi, G. Wang, Y. Yan, S. Mei, and T. Luo, "Effect of rotating twisted tape on thermo-hydraulic performances of nanofluids in heat-exchanger systems," *Energy Convers. Manag.*, vol. 166, pp. 744–757, 2018.

[26] N. T. R. Kumar, P. Bhramara, A. Kirubeil, L. S. Sundar, M. K. Singh, and A. C. M. Sousa, "Effect of twisted tape inserts on heat transfer, friction factor of Fe3O4 nanofluids flow in a double pipe U-bend heat exchanger," *Int. Commun. Heat Mass Transf.*, vol. 95, pp. 53–62, 2018.

[27] P. Samruaisin, W. Changcharoen, C. Thianpong, V. Chuwattanakul, M. Pimsarn, and

S. Eiamsa-ard, “Influence of regularly spaced quadruple twisted tape elements on thermal enhancement characteristics,” *Chem. Eng. Process. Intensif.*, vol. 128, pp. 114–123, 2018.

[28] K. Ruengpayungsak, A. Saysroy, K. Wongcharee, and S. Eiamsa-Ard, “Thermohydraulic performance evaluation of heat exchangers equipped with centrally perforated twisted tape: Laminar and turbulent flows,” *J. Therm. Sci. Technol.*, vol. 14, no. 1, pp. JTST0002–JTST0002, 2019.

[29] Y. Hong, J. Du, and S. Wang, “Experimental heat transfer and flow characteristics in a spiral grooved tube with overlapped large/small twin twisted tapes,” *Int. J. Heat Mass Transf.*, vol. 106, pp. 1178–1190, 2017.

[30] Y. Hong, J. Du, and S. Wang, “Turbulent thermal, fluid flow and thermodynamic characteristics in a plain tube fitted with overlapped multiple twisted tapes,” *Int. J. Heat Mass Transf.*, vol. 115, pp. 551–565, 2017.

[31] A. Hasanpour, M. Farhadi, and K. Sedighi, “Intensification of heat exchangers performance by modified and optimized twisted tapes,” *Chem. Eng. Process. Intensif.*, vol. 120, pp. 276–285, 2017.

[32] M. H. Esfe, H. Mazaheri, S. S. Mirzaei, E. Kashi, M. Kazemi, and M. Afrand, “Effects of twisted tapes on thermal performance of tri-lobed tube: an applicable numerical study,” *Appl. Therm. Eng.*, vol. 144, pp. 512–521, 2018.

[33] S. Rashidi, M. Akbarzadeh, N. Karimi, and R. Masoodi, “Combined effects of nanofluid and transverse twisted-baffles on the flow structures, heat transfer and irreversibilities inside a square duct–A numerical study,” *Appl. Therm. Eng.*, vol. 130, pp. 135–148, 2018.

[34] M. Muralidhara Rao and V. M. K. Sastri, “Experimental investigation for fluid flow and heat transfer in a rotating tube with twisted-tape inserts,” *Heat Transf. Eng.*, vol.

16, no. 2, pp. 19–28, 1995.

[35] C. Yang, A. Nakayama, and W. Liu, “Heat transfer performance assessment for forced convection in a tube partially filled with a porous medium,” *Int. J. Therm. Sci.*, vol. 54, pp. 98–108, 2012, doi: https://doi.org/10.1016/j.ijthermalsci.2011.10.023.

[36] H. Arasteh, R. Mashayekhi, D. Toghraie, A. Karimipour, M. Bahiraei, and A. Rahbari, “Optimal arrangements of a heat sink partially filled with multilayered porous media employing hybrid nanofluid,” *J. Therm. Anal. Calorim.*, pp. 1–14, 2019.

[37] T. Davood, M. Ramin, A. Hossein, S. Salman, N. Mohammadreza, and C. A. J., “Two-phase investigation of water-Al2O3 nanofluid in a micro concentric annulus under non-uniform heat flux boundary conditions,” *Int. J. Numer. Methods Heat Fluid Flow*, vol. 30, no. 4, pp. 1795–1814, Jan. 2019, doi: 10.1108/HFF-11-2018-0628.

[38] ANSYS, Inc. (2018) Ansys Fluent User's Guide, Release 18.0.

[39] M. Ghalambaz, R. Mashayekhi, H. Arasteh, H. M. Ali, P. Talebizadehsardari, and W. Yaïci, “Thermo-Hydraulic Performance Analysis on the Effects of Truncated Twisted Tape Inserts in a Tube Heat Exchanger,” *Symmetry (Basel).*, vol. 12, no. 10, p. 1652, 2020.

[40] M. Ghalambaz, H. Arasteh, R. Mashayekhi, A. Keshmiri, P. Talebizadehsardari, and W. Yaïci, “Investigation of Overlapped Twisted Tapes Inserted in a Double-Pipe Heat Exchanger Using Two-Phase Nanofluid,” *Nanomaterials*, vol. 10, no. 9, p. 1656, 2020.

[41] M. Ghaneifar, H. Arasteh, R. Mashayekhi, A. Rahbari, R. Babaei Mahani, and P. Talebizadehsardari, “Thermohydraulic analysis of hybrid nanofluid in a multilayered copper foam heat sink employing local thermal non-equilibrium condition: Optimization of layers thickness,” *Appl. Therm. Eng.*, vol. 181, p. 115961, 2020, doi: https://doi.org/10.1016/j.applthermaleng.2020.115961.

[42] L. Wei, H. Arasteh, A. Parsian, M. Taghipour, R. Mashayekhi, and I. Tlili, “Locally

weighted moving regression: A non-parametric method for modeling nanofluid features of dynamic viscosity," *Phys. A Stat. Mech. its Appl.*, p. 124124, 2020.

[43] L. S. Sundar and K. V Sharma, "An experimental study on heat transfer and friction factor of Al2O3 nanofluid," *J. Mech. Eng. Sci.*, vol. 1, pp. 99–112, 2011.